Colloid Polym Sci (2007) 285:1561–1571
DOI 10.1007/s00396-007-1726-5

ORIGINAL CONTRIBUTION

The mechanism of pyrene fluorescence quenching by selective and nonselective quenchers during sol–gel transition

Ewa Miller · Donata Jóźwik-Styczyńska

Received: 5 March 2007 / Revised: 22 May 2007 / Accepted: 18 June 2007 / Published online: 10 August 2007

Abstract The process of pyrene fluorescence quenching by potassium iodide, acrylamide, and gaseous oxygen in silane sol during sol–gel transition was investigated. Pyrene fluorescence emission spectra were recorded vs concentrations of the added quencher on consecutive days of the gelling process. When using 0, 20, and 100% oxygen in the gas mixture as a quencher, time-resolved measurements were also made. On this basis, Stern–Volmer constants were determined on consecutive days of the gelling process, availability of fluorophore molecules to the quencher, and also rate constants of pyrene quenching by acrylamide, iodide ions, and oxygen were specified. Moreover, diffusion coefficients were determined for acrylamide and potassium iodide in the silane gel formed. The mechanism of fluorophore quenching in sol of growing viscosity and in gel was discussed in view of using this carrier in the construction of sensors and optical biosensors.

Keywords Fluorescence quenching · Sol–gel transition · Pyrene

Introduction

As a result of gelling silane monomers such as TEOS and TMOS, transparent, chemically and mechanically stable glassy materials are formed. Therefore this sol–gel method for obtaining a gel carrier is one of the most attractive methods used presently to synthesize nonorganic carriers to be used in optical materials [1, 2]. Besides, when using this method, it is possible to change the gel lattice structure and both distribution and size of pores, depending on such factors as input sol composition, the type of monomer hydrolysis, and temperature. Contrary to high-temperature synthesis of 96% silica glass, from the point of view of the applications of silane matrices, a significant advantage are very mild conditions of gelling, i.e., room temperature and duration from several minutes to several hours. Hence, organic compounds, e.g., enzyme and luminescence probe, introduced to the input sol are not destroyed, deactivated, or degraded during the gelling process. Therefore, silane gels could find applications also as carriers in the construction of sensors and optical biosensors [3–5].

The use of a silane gel with a fluorophore in the optical sensor is related to immobilization of this carrier on the end of the optical fiber [6–10]. When a gel lattice is formed, the polymer structure changes, pores filled with water, and ethanol mixture are formed, and connections between cavities appear. The rate at which substrate molecules diffuse through the gel layer to a probe immobilized in the gel has a significant influence on the response time of the sensor. Hence, it seems interesting to assess the accessibility of the fluorophore or enzyme immobilized in a silane gel, which reflects the location of the molecules in the porous matrix. Changes of micropolarity in the nearest vicinity of the probe in the gel pores can be determined using, for instance, pyrene whose fluorescence emission spectrum depends on the ambient polarity [11]. Many studies describe the quenching of the fluorescence of a probe immobilized in the gel by selected quenchers [12–14]. In this case, the character of quenching, which is either dynamic or static, and the Stern–Volmer constant determined from existing models enable the estimation of the number and type of centers formed by the fluorophore molecules in the gel pores and the accessibility

E. Miller (✉) · D. Jóźwik-Styczyńska
Institute of General Food Chemistry,
Technical University of Łódź,
ul. Stefanowskiego 4/10,
90-924 Łódź, Poland
e-mail: emiller@snack.p.lodz.pl

of the fluorophore and/or enzyme molecules immobilized in a gel carrier to the diffusing substrate molecules. This information is particularly useful when a thin gel layer is formed on the fiber surface in the optical sensor, because the thickness and structure of the gel layer affect notably the sensor operation: its response time and the range of tested substrate concentration [15].

In this study, the quenching of pyrene by selected quenchers is monitored on consecutive days as the silane monomer (tetraethylorthosilane [TEOS]) undergoes gellation. The sol–gel process was carried out with the use of acid hydrolysis. Potassium iodide, acrylamide, and gaseous oxygen were used as quenchers. The pyrene fluorescence emission spectra were recorded both in the input sol as the viscosity increased and also in the gel as a function of quencher concentration. When oxygen was used, the kinetics of the pyrene fluorescence decay was also recorded as a function of gas content in the sample. Based on the considered quenching mechanisms, the accessibility of the fluorophore molecules entrapped in the gel to selected chemicals diffusing in the gel lattice was discussed [16, 17].

Experimental

The input sol contained TEOS, ethanol, and water in the molar ratio 1:6:6, respectively. Pyrene (Aldrich) purified by recrystallization from ethanol, TEOS (Sigma), spectrally pure ethanol, and hydrochloric acid (P.O.Ch., Gliwice, Poland) as well as distilled and deionized water were used in the experiments. Pyrene at a concentration of 10^{-6} M in ethanol was added to the sol. The value of pH in the sol was measured using a pH meter, by addition of a relevant amount of concentrated hydrochloric acid. The sol was mixed for 2 h and was then divided into four equal portions, which corresponded to four consecutive days of gelation. The sol portions were placed in four quartz measuring cuvettes closed with a rubber stopper with two needles. On subsequent days, the selected sol was deaerated by transferring gaseous nitrogen through the sample for 20 min. Next, the needle holes were closed with plugs. On consecutive days of the process, 5 μl of 0.9 M potassium iodide or 0.9 M acrylamide in aqueous solution was added through one of the needles to selected sol. Each sample was mixed, and the excitation and emission spectra of the pyrene fluorescence in the sol were recorded. Both the sol, whose viscosity was increasing on consecutive days of the gelling process, and the gel were transparent. No scattered light correction was used because the authors were interested in relative changes of pyrene fluorescence emission in the presence of a quencher at various stages of the gelling process of the same sample. Hence, experimental data are given in the form of relative values, e.g., I_0/I.

To determine the parameters describing the quenching of pyrene by oxygen for the sol–gel transition, the following gases: nitrogen, oxygen, or previously prepared mixture of oxygen and nitrogen were transferred for 20 min at a constant rate through the sol sample, which was corresponding to a consecutive day of the gelation process. Next, the pyrene fluorescence emission or decay curve was recorded. The mixtures of gaseous oxygen and nitrogen of appropriate composition were prepared in a separate empty cylinder, which was filled with pure gases at relevant pressures. To determine the rate constants for the quenching of pyrene entrapped in the gel and the diffusion constants for acrylamide and potassium iodide in the gel, the gelled carrier in the measuring cuvette was flushed with 70 μl of the selected quencher solution, which corresponded to the total volume of the quencher applied. Next, fluorescence emission spectra of the probe were recorded in time. Measurements were carried out at room temperature, keeping the samples at 20 °C. Steady state measurements of fluorescence were made using a Fluoromax-2 spectrofluorimeter (Jobin Yvon), and lifetimes of the probe emissions were recorded by a single photon-counting system (Edinburgh Analytical Instruments—FL 900CDT).

Results and discussion

Acrylamide

The silane sol prepared for tests was poured into four identical cuvettes. A neutral quencher-acrylamide was added stepwise to the deaerated sol in the cuvette at a given day of the gelation. The assumption was that the gelling process was identical in each cuvette. After adding each acrylamide aliquot, the pyrene excitation and emission fluorescence spectra in the sol were recorded (Fig. 1a,b). Each day, a decrease in intensity of the pyrene fluorescence emission as a function of quencher concentration was observed during the sol–gel transition. Results are given as a classic Stern–Volmer plot in Fig. 2a. The trends obtained on the first and second day of gelation were straight lines. This proves that, in the sol, there is one type of pyrene molecules, which is fully accessible for quenching by acrylamide. Hence, to estimate the process of quenching on the first and second day of gelation, the classic Stern–Volmer relation 1 could be used:

$$I_0/I = 1 + K_{S-V}[Q] \quad (1)$$

where:

I_0 initial intensity of pyrene fluorescence in the absence of acrylamide molecules,

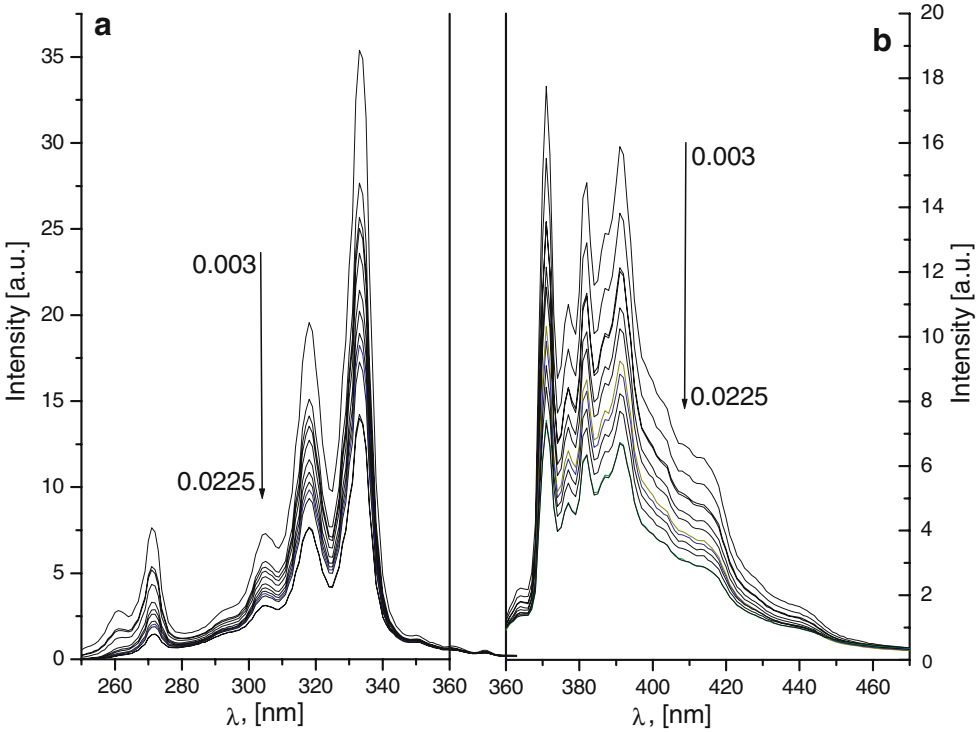

Fig. 1 Fluorescence excitation (**a**) and emission (**b**) spectra for pyrene quenching by acrylamide in silane sol on the first day of gelation; λ_{ex}=337 nm, λ_{em}= 392 nm, $c_{Py}=5\cdot10^{-7}$ M, c_{AC}= 0.9 M; c_{AC} in the sample after adding consecutive portions of the quencher: 0.0015–0.0224 M

I intensity of pyrene fluorescence quenched by acrylamide,
$[Q]$ acrylamide concentration, (M)
K_{S-V} Stern–Volmer constant, (M^{-1})

On the third and fourth day of the sol–gel transition, the trends became nonlinear (Fig. 2a). Such results suggest that, in the sol with increasing viscosity, particularly near the percolation threshold, the fluorophores have different

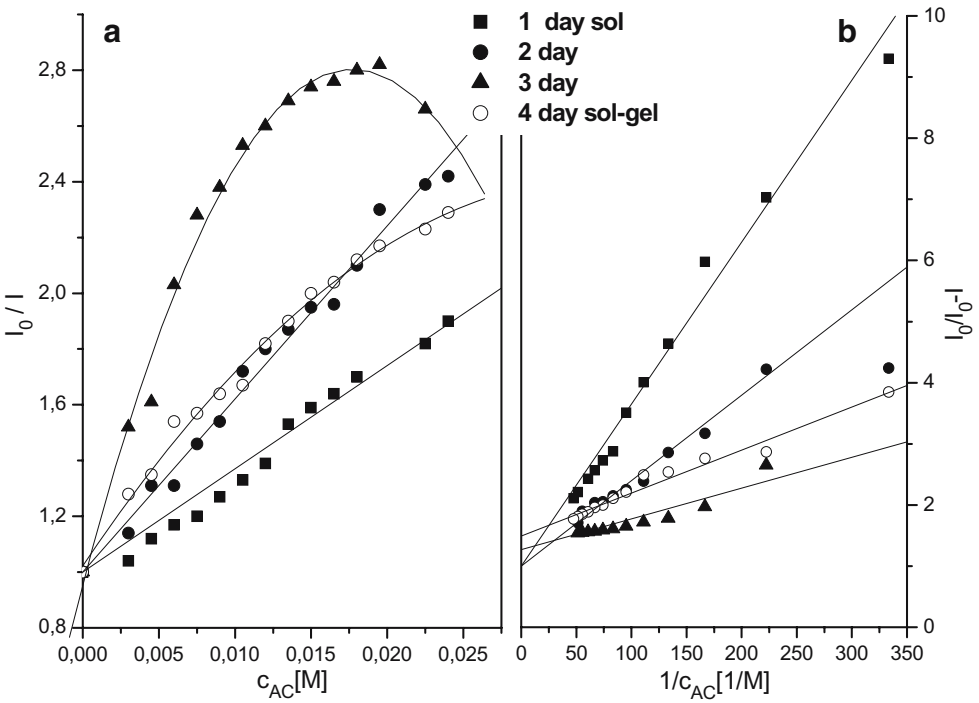

Fig. 2 Stern–Volmer plots (**a**) and modified Stern–Volmer plots (**b**) of the quenching by acrylamide of the pyrene emission in silane sol on the consecutive days of gelation

accessibility to the quencher. To determine the Stern–Volmer constant, a multisite model simplified by Demas et al. [13] into a two-site model (2) was used. In this model, two types of fluorophores are assumed to have a different microenvironment and, consequently, different degrees of accessibility to acrylamide molecules.

$$I_0/I = \left[\frac{f_1}{1 + K_{SV1}[Q]} + \frac{f_2}{1 + K_{SV2}[Q]}\right]^{-1} \quad (2)$$

where:

f_1, f_2 substrate accessibility to the first and second type of fluorophore sites
K_{sv1}, K_{sv2} Stern–Volmer constants for quenching of the first and second type of fluorophore sites, respectively
I_0, I, $[Q]$ as in Eq. 1

Assuming that f_2=0 (Lehrer model [13]), Eq. 2 simplifies to Eq. 3:

$$I_0/I = \left[\frac{f_1}{1 + K_{SV1}[Q]}\right]^{-1} \quad (3)$$

Assuming that $\Delta I = I_0 - I$, Eq. 3 is transformed into Eq. 4:

$$I_0/\Delta I = 1/f_1 + 1/f_1 \cdot 1/K_{S-V1} \cdot 1/[Q] \quad (4)$$

where:

K_{sv1} Stern–Volmer constant determined for available fluorophore molecules, (M^{-1})
$[Q]$ acrylamide concentration, (M)
f_1 availability to one type of pyrene centers

Next, experimental data describing the quenching of pyrene by acrylamide on consecutive days of sample gelation (Fig. 2a) were presented as modified Stern–Volmer plots in Fig. 2b using Eq. 4. The relation $I_0/\Delta I$ vs I/c_{AC} was linear, and the Lehrer model [13] was applied for protective quenching on the third and fourth day of gelation.

The constants K_{sv} were determined for the first 2 days of silane sol gelation with Eq. 1, while for the third and fourth day of the process, K_{sv} was calculated with Eq. 4. Equations 1 and 4 were also used to determine the accessibility of the fluorophores to acrylamide on the consecutive days of the process (Table 1). Analysis of the data in Table 1 shows that the Stern–Volmer constant increases with increasing time. In parallel, a decrease in the fraction of accessible fluorophore—pyrene to acrylamide molecules—was recorded. For comparison, the values of the Stern–Volmer constant determined for pyrene in homogenous solutions of cyanomethane, quenched by the derivatives of aliphatic and aromatic amines, are 200–300 (M^{-1}) [16]. On the other hand, for pyrene immobilized covalently in the silane gel, K_{sv} increases or decreases several times, depending on the method of gel formation (either acidic or alkaline), which controls the density and size of the pores being formed [16, 18].

When analyzing the results obtained on consecutive days of the gelation process, changes in a micro- and macro-system should be considered. The changes refer to an increase in the viscosity of the medium particularly near the percolation threshold and stiffening of the matrix caused by the formation of a stiff gel lattice [2].

To describe in detail the mechanism of the quenching of pyrene in the silane sol by acrylamide, the bimolecular quenching rate constant k_{qAC} was determined (Table 1). The constant was calculated from Eq. 5 using $\hat{\tau}_0$, the weight average pyrene lifetime, which was calculated from the pyrene lifetimes τ_0 in the deaerated silane sol on consecutive days of sample gelling. The pyrene lifetimes were determined from time-resolved fluorescence measurements (Table 3):

$$K_{sv} = k_q \cdot \hat{\tau}_0 \quad (5)$$

where:

K_{sv} Stern–Volmer constant, (M^{-1})
k_q bimolecular quenching rate constant, ($M^{-1}s^{-1}$)
$\hat{\tau}_0$ weight average lifetime of pyrene in the deaerated sample on the consecutive days of gelation process, (ns)

The values of k_q in Table 1 are of the order of 10^9 (M^{-1}, s^{-1}). During gelation, an increase in k_q is observed, particularly near the percolation threshold (Table 1). Typical k_q values for diffusion-controlled quenching are of the order 10^{10} M^{-1} s^{-1} [19]. Higher values of k_q usually refer to environments where additional interactions occur between the fluorophore and quencher molecules, e.g., hydrogen bond and complex formation. Lower values of k_q suggest that quenching is restricted by steric hindrance until conditions are reached where the reaction rate is controlled by diffusion [4].

Sun et al. [14] observed an increase in the pyrene quenching rate constant k_q from 2.0 to 2.8 10^9 M^{-1} s^{-1} or 8.0 to 12.0 10^9 M^{-1} s^{-1} when pyrene was quenched by neutral quenchers: nitromethane and dinitrobenzene in water solutions of polyanion acrylamide copolymers. The value of k_q increased with increasing density of the polymer fraction when the negative charges of the products of condensation were neutralized by protons of the solvent. Only prolongation of the polymer condensation time induced a further increase in the aggregation of macromolecules, which caused that a total negative charge

Table 1 Stern–Volmer constants for pyrene quenched by iodide ions, acrylamide, and oxygen on consecutive days of sol–gel transition, determined on the basis of steady-state measurements

Days	Quencher										
	Acrylamide				Potassium iodide				Oxygen		
	K_{sv} (M^{-1})	R^2	f_a	k_q (M^{-1} s^{-1}) 10^{-9}	K_{sv} (M^{-1})	R^2	f_a	k_q (M^{-1} s^1) 10^{-9}	K_{sv} ($\%^{-1}$)	R^2	k_q ($\%^{-1}$ s^{-1}) 10^{-5}
1 sol	37.7	0.993	1	0.25	59.3	0.985	1	0.40	0.16	0.997	11.0
2 sol	71.5	0.994	1	0.56	99.9	0.993	1	0.78	0.15	0.993	11.8
3 sol	252.5	0.998	0.79	3.16	128.5	0.996	1	1.61	0.16	0.949	20.3
4 sol–gel	211.6	0.994	0.67	3.64	508.6	0.978	0.70	6.89	0.13	0.981	22.0

$K_{sv}=k_q\cdot\hat{\tau}_0$; $\hat{\tau}_0$, weight average pyrene lifetime on a given day of the gelling process without a quencher (ns); k_q, bimolecular quenching rate constant (M^{-1} s^{-1})

appeared in the polymer. This in turn caused a decrease in accessibility to the quencher and a decrease in k_q.

Results of the pyrene quenching by acrylamide observed during gelation (Table 1) are a consequence of a fundamental change in the microenvironment of the fluorophore and quencher because of the formation of a rigid system in the form of a gel lattice. As a result of competing reactions of hydrolysis and condensation, silane oligomers are formed in the gelation process; the quantity and size of the oligomers increase remarkably near the sol–gel transition [18]. Hence, viscosity of the sol increases until the formation of a gel lattice structure whose pores are filled with a liquid phase, i.e., water–ethanol mixture. These aggregates temporarily protect some of the fluorophores from quenching by acrylamide. An increase in the system rigidity resulting in polymer lattice formation causes most probably an increase in the local fluorophore concentration in the regions accessible to the quencher, e.g., in big gel pores. Pyrene molecules placed in big gel cavities are surrounded by water and ethanol molecules, where they are more exposed to and quenched faster by acrylamide (Table 1).

Potassium iodide

A similar experiment was carried out for the TEOS gelling process, using iodide ions as a selective, ionic quencher of pyrene. The quencher was selected to access and quench fluorophores present in the mixture of polar solvents (water–alcohol) and hydrolyzing silane monomer. The quencher was to imitate the molecule of a substrate with a negative charge, which was supplied to the sol. The fluorophore was placed in the input silane sol, which was divided into four portions as previously done. The portions corresponded to four consecutive days of gelation. The pyrene fluorescence excitation and emission spectra were recorded after the addition of potassium iodide to the sol (Fig. 3a,b). Experiments were conducted on the consecutive days of gelation for the sol using a different cuvette each day (Fig. 4a). On the first 3 days of gelation, the I_0/I ratio increased linearly with quencher concentration. K_{svI} for pyrene quenching in the sol on these days was determined using the classical Stern–Volmer Eq. 1. On the fourth day, the sample gelled, and a nonlinear trend was recorded. As in the case of acrylamide, the experimental data were treated by plotting the $I_0/\Delta I$ ratio as a function of $1/[c_{KI}]$ (Fig. 4b). For the data on the fourth day of gelation, a linear relation in the whole range of applied concentrations of iodide ions was obtained. To determine the Stern–Volmer constant, Lehrer's modified two-site model (4) could be used, which assumes the inaccessibility of the two fluorophore populations. Values of the determined constants are given in Table 1. K_{svI} increased gradually on consecutive days of gelation, while on the day when the gelation was completed, an abrupt nearly fourfold increase was observed. Except for the values calculated for the third day of gelation, the obtained values were higher than when acrylamide was used as a quencher. The fraction of accessible fluorophores read from the diagram of $I_0/\Delta I$ as a function of $1/[c_{KJ}]$ on the fourth day was smaller than unity reaching 0.70. For comparison, K_{svI} determined for pyrene in the acetonitrile solution was 89.6 [M^{-1}] [20].

Using the K_{svI} value calculated for pyrene during the sol–gel transition and the weight average lifetimes of pyrene $\hat{\tau}_0$ calculated from the pyrene lifetimes τ_0 in the deaerated sol, the bimolecular quenching rate constants k_q were also determined (Table 1 according to Eq. 5). For comparison, k_q determined for pyrene using methyl iodide in methylcyclohexane solutions equaled 4.1 and $1.9\cdot10^7$ M^{-1} s^{-1} for the pyrene monomer and excimer, respectively [21]. When analyzing the quenching of a probe incorporated in a heterogeneous medium by ionic quenchers, both the quencher load and character of the microenvironment in the form of a polymer gel lattice should be considered. For example, Sun

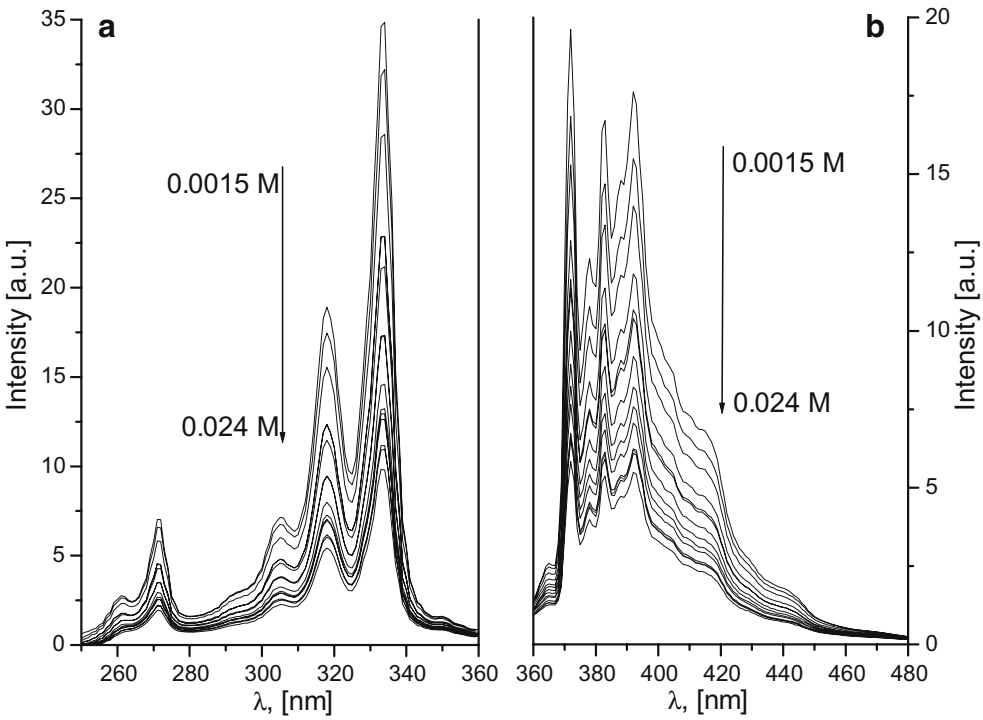

Fig. 3 Fluorescence excitation (**a**) and emission (**b**) spectra for pyrene quenching by potassium iodide in silane sol on the first day of gelation; λ_{ex}=337 nm, λ_{em}=392 nm, $c_{Py}=5\cdot10^{-7}$ M, c_{KI}=0.9 M; c_{KI} in the sample after adding consecutive portions of the quencher: 0.0015–0.024 M

et al. [14] used Cu^{2+} and I^- ions to quench pyrene attached onto an anionic acrylamide copolymer. They observed that an increase in the polymer fraction resulted in an increase in pyrene quenching by copper ions. The authors related this effect to an increased condensation of the Cu^{2+} cations onto the polyanion. Iodide ions produced the opposite result. An increase in polyanion chain density caused a decrease in pyrene fluorescence quenching by these ions, because of electrostatic repulsion of the quencher anion by the polyanion. Similarly, nearly seven times higher quenching rate of pyrene dissolved in acetonitrile by Tl^{+1} (621.9 M^{-1}) than by iodide ions (89.6 M^{-1}) was reported [20].

In the input silane sol, the fluorophore molecules are surrounded by polar molecules of water and ethanol and silane monomer. The polymer chains of gel being formed are composed of siloxane groups -0-Si-0- and silanol groups -Si-

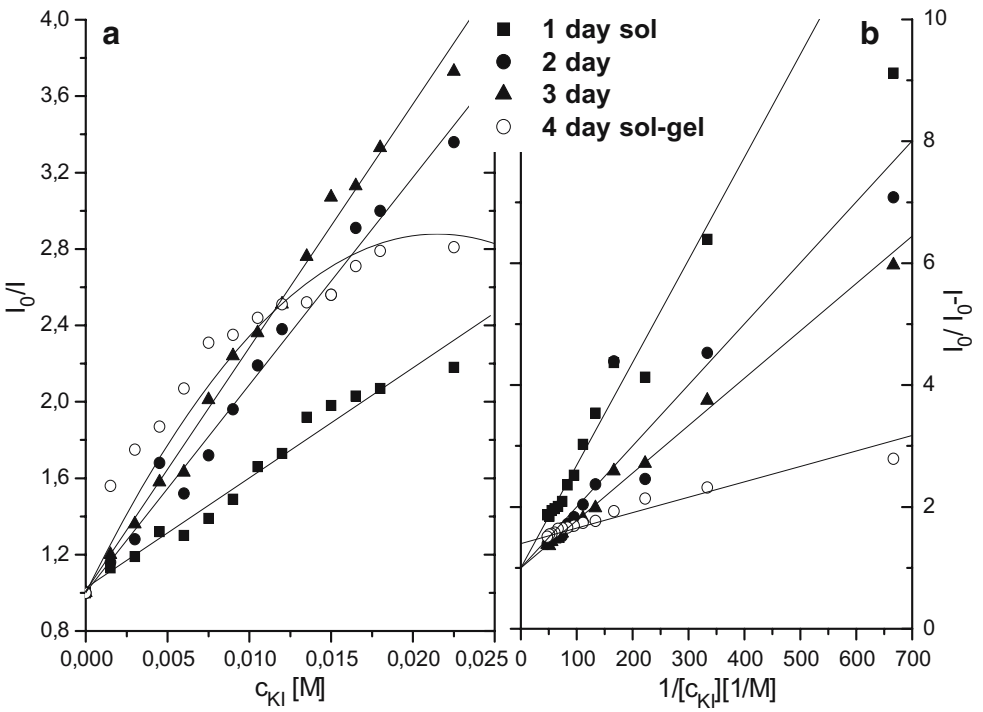

Fig. 4 Stern–Volmer plots (**a**) and modified Stern–Volmer plots (**b**) of the quenching by potassium iodide of pyrene emission in silane sol on the consecutive days of gelation

0H, directed to the inside of the pores, not used in the condensation of silane monomers. The phenomenon of water molecules adsorption on gel pore surface is also known [13]. Most probably, the polar microenvironment of hydrophobic pyrene molecules and also restricted, polar inner surface of gel cavities enhance slightly the process of quenching by the negatively charged iodide ions, as compared to pyrene quenching by acrylamide in the same conditions.

An attempt was also made to determine the quenching kinetics of pyrene placed in the pores of the existing gel by means of iodide ions and acrylamide. For this purpose, the fluorescence emission spectra of pyrene in the gel formed in the cuvette were recorded because the moment of flooding the gel surface with a solution of potassium iodide or acrylamide. The quenching process was handled by the first-order kinetics (Fig. 5). The following stages of fluorophore emission quenching in the gel were distinguished: up to 3 h in the case of acrylamide and to 4 h and longer than 4 h for potassium iodide. The determined quenching rate constants are given in Table 2. Having the relation:

$$\frac{I_0 - I_t}{I_0 - I_\infty} = \frac{4}{L}\left[\frac{Dt}{\pi}\right]^{1/2} \tag{6}$$

I_0 intensity of pyrene fluorescence emission in time $t=0$
I_t intensity of pyrene fluorescence emission after time t
I_∞ intensity of pyrene fluorescence emission after infinitely long time
L distance between gel surface and measuring window, 1.5 cm was assumed
D diffusion coefficient, (cm^2/s)
t diffusion time, (s)

based on the recorded pyrene fluorescence emission spectra after adding subsequent portions of acrylamide, the ratio $(I_0 - I)/(I_t - I_\infty)$ was plotted as a function of $t^{1/2}$ in the interval of 0–3 h. From the slope of the linear relation $y=0.00106\times(R=0.904)$, the quencher diffusion coefficient D equal to $0.49\cdot10^{-6}$ (cm^2/s) was determined for pyrene. Similarly, plots of $(I_0 - I)/(I_t - I_\infty)$ for quenching by iodide were prepared as a function of $t^{1/2}$ in the interval of 0–4 h and 4–7.5 h. The obtained straight lines $y=0.00161\times(R=0.901)$ and $y=0.01119\times(R=0.995)$ yielded the diffusion coefficients 1.145 and $55.29\cdot10^{-6}$ (cm^2/s), respectively (Table 2).

When analyzing the results and comparing them with the results obtained by other authors, we should take into account experimental conditions, i.e., the application of gel formed into a block in the cuvette (a cubicoid of base 1 cm^2 and height of 3 cm), whose surface (1 cm^2) in the instant of starting the experiment was flooded with a quencher of given volume. The emission signal of pyrene fluorescence in the gel was recorded approximately in the middle of the cuvette height because of the apparatus construction. Based on the diffusion coefficient determined for the quenching of pyrene by acrylamide and potassium iodide (Table 2), the

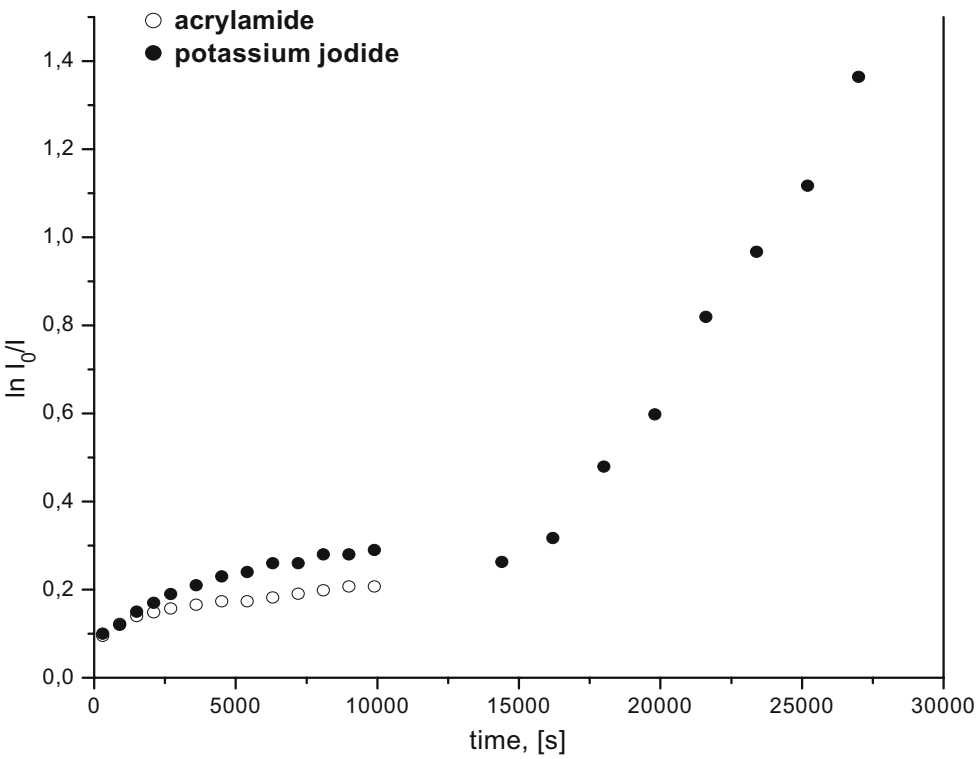

Fig. 5 Kinetics of pyrene quenching in silane gel by: *open circles*, acrylamide; *closed circles*, potassium iodide; $c_{Py}=5\cdot10^{-7}$ M, other experimental data in "Experimental"

Table 2 Rate constants of pyrene quenching by selected quenchers in silane gel

Quencher	Pyrene quenching rate constants and diffusion constants in gel			
	$k_1(s^{-1})\ 10^5$	$D_1(cm^2/s)\ 10^6$	$k_2(s^{-1})\ 10^5$	$D_2(cm^2/s)\ 10^6$
Iodide ions	2.2	1.15	9.0	55.29
Acrylamide	3.1	0.49	–	–

fluorophore quenching process in the silane gel is controlled by diffusion and takes place at a comparable rate for both quenchers. Diffusion coefficients of these quenchers determined in the silane gel have values similar to those found in solutions.

Oxygen

Steady-state and time-resolved fluorescence measurements of pyrene in silane sol as a function of the concentration of oxygen dissolved in the sol were carried out on the consecutive days of sol–gel transition until the sample was gelled. Zero percent of oxygen concentration was obtained as a result of passing gaseous nitrogen through the sol in the cuvette. One hundred percent of oxygen content corresponded to sample exposed to pure gaseous oxygen in the same time, 20% was obtained when air was passed through the sample, while 10, 30, and 50% oxygen was a result of passing through the sol a mixture of gases prepared earlier in a separate cylinder. Examples of fluorescence emission spectra of pyrene quenched by oxygen dissolved in sol are shown in Fig. 6a. Based on the steady-state measurements of pyrene emission, the trends shown in Fig. 6b were obtained on the consecutive days of gelation. Significant changes such as a decrease in pyrene emission intensity in the sample were observed between 0 and 50% oxygen content in the sol. Similar changes were observed on the consecutive days of the process, irrespective of the increasing sol viscosity during the sol–gel transition. The Stern–Volmer constant was determined from the classical Eq. 1 and presented in Table 1. K_{sv} assumes similar values on all days until the gel has been formed. This is an evidence of similar pyrene quenching by oxygen during gelation, with preservation of full accessibility of pyrene to oxygen, surrounded by water and ethanol molecules in the gel being formed.

To explain the mechanism of pyrene quenching by gaseous oxygen for the sol–gel transition, time-resolved fluorescence measurements were also performed. The fluorescence decay of pyrene were recorded on consecutive days of gelation for different content of oxygen in the sol. The decays were multiexponential (Fig. 7a,b). Therefore, they were fitted using Lehrer's model by means of a two-exponential equation with two decay times, τ_1 and τ_2:

$$I(t) = A_1 \exp(-t/\tau_1) + A_2 \exp(-t/\tau_2) \quad (7)$$

where: τ_1, τ_2—pyrene lifetimes corresponding to two different microenvironments of probe molecules.

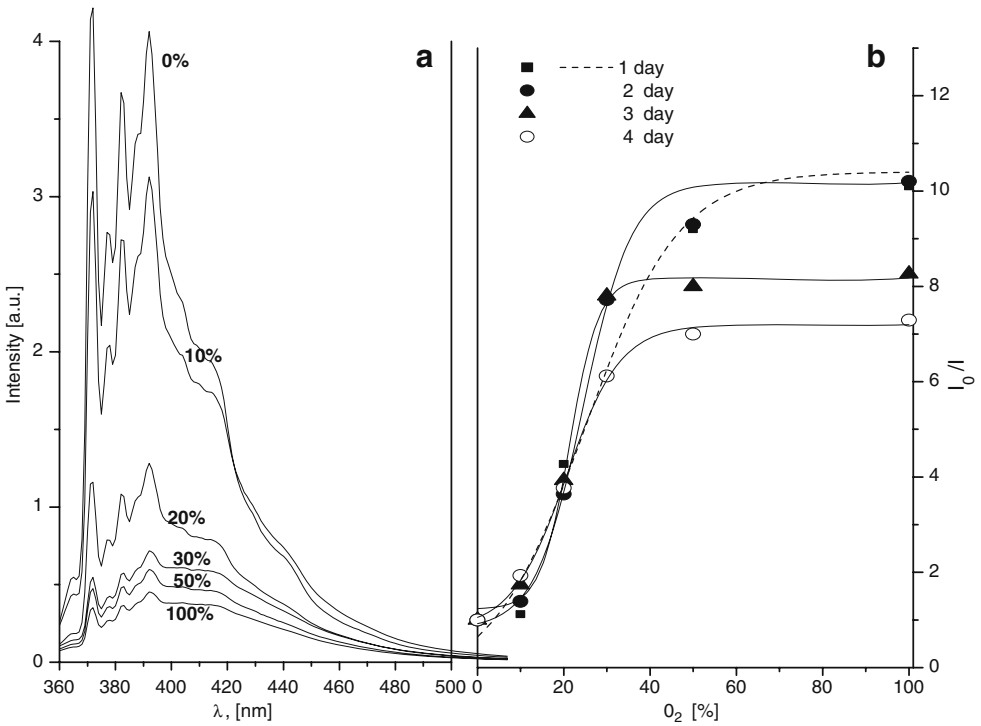

Fig. 6 **a** Emission spectra of pyrene quenched by oxygen in silane sol on the second day of gelation; **b** Stern–Volmer plot for pyrene emission in silane sol quenched by oxygen during sol–gel transition; 0, 20, and 100%—gaseous nitrogen, air, and oxygen was transferred through the sol, respectively. A gaseous mixture of nitrogen and oxygen prepared earlier in a cylinder was transferred through the sol—10, 30, and 50% oxygen

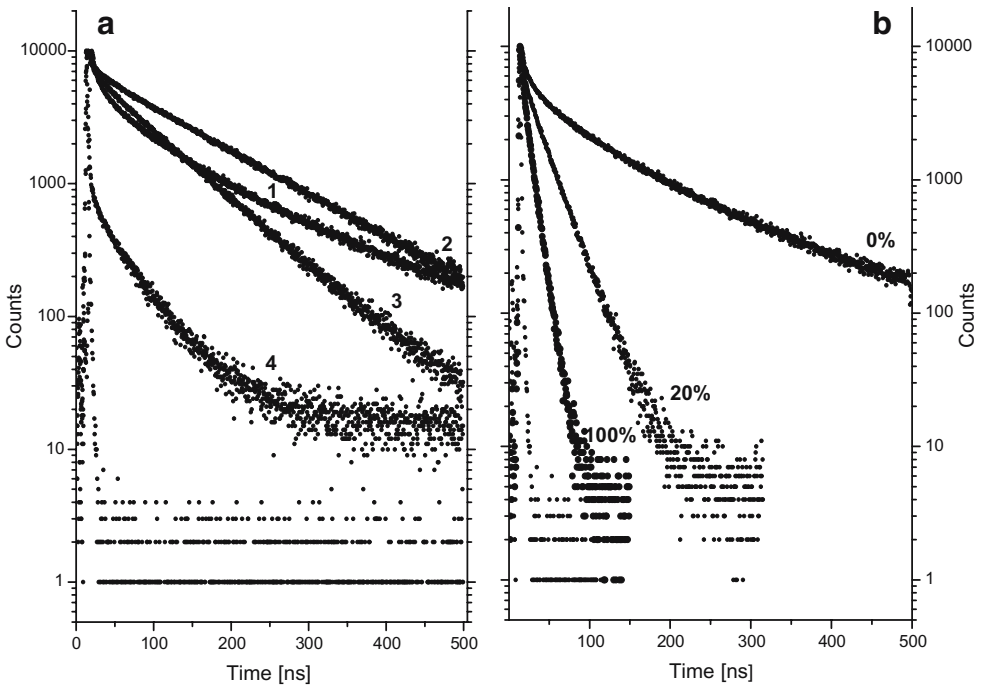

Fig. 7 **a** Kinetics of fluorescence decay of pyrene in silane sol on the consecutive days of gelation for 0% oxygen in sol: *1*—first day (sol), *2*—second day (sol), *3*—third day (sol), *4*—fourth day (sol–gel); **b** kinetics of fluorescence decay of pyrene vs oxygen concentration in input sol

Results from the fits are given in Table 3. The two determined lifetimes of pyrene differ significantly. A dominant one (97%) τ_1 equals 150 ns in anaerobic conditions. τ_1 is characteristic of the monomer form of pyrene in the sol, while the second lifetime τ_2, is equal to a few nanoseconds. During the gelation process with 0% oxygen, a shortening of the lifetimes τ_1 and τ_2 is observed. The preexponential weight of the exponential with the shorter decay time τ_2 increases at the cost of τ_1. Hence, a conclusion can be drawn that τ_2 is most probably responsible for the interaction between a probe molecule and silanol groups created in the newly forming gel and even for the adsorption of fluorophore on the surface of pores in the formed gel. Addition of oxygen (Table 3, 20%) to the sol causes quenching of pyrene fluorescence and remarkable shortening of decay time τ_1 to 26 ns. This decay time does not change on the consecutive days of the gelation process. Only when the gel forms is τ_1 shortened to about 19 ns. This effect is a result of additional quenching of pyrene fluorescence emission because of the interaction of the fluorophore with the gel lattice. The above results confirm the previous steady-state fluorescence measurements from which it followed that accessibility of pyrene molecules for a gaseous quencher is not decreased. A further increase in oxygen content in the sol (Table 3, 100%) causes another shortening of the decay time τ_1 from 26 to 10 ns and remains unchanged until a gel is formed. This is a result of a maximum quenching of pyrene fluorescence in the sol under the influence of pure oxygen.

Both in the case of longer and shorter pyrene lifetime on the consecutive days of gelation a dependence on quencher concentration was found, which provided an evidence of dominating dynamic character of the quenching process.

Table 3 Pyrene lifetime on consecutive days of gelation vs the concentration of oxygen transferred through the sample

0_2 in gas mixture (%)	Lifetime (ns)	Sol–gel transition [days]											
		1 (sol)			2 (sol)			3 (sol)			4 (sol–gel)		
		τ (ns)	(%)[a]	$\chi 2$	*τ (ns)*	(%)[a]	$\chi 2$	*τ (ns)*	(%)[a]	$\chi 2$	*τ (ns)*	(%)[a]	$\chi 2$
0	τ_1	151.5	96.7	1.4	129.6	97.8	1.7	82.6	95.5	1.6	73.8	77.7	1.9
	τ_2	5.3	3.3		7.3	2.2		4.7	4.5		1.9	22.3	
20	τ_1	26.1	89.8	1.2	28.9	92.2	1.2	29.1	89.7	1.3	18.6	85.3	1.5
	τ_2	4.8	10.2		5.4	7.8		6.1	10.3		2.0	14.7	
100	τ_1	10.5	72.3	1.2	11.3	81.4	1.4	9.5	76.4	1.9	10.6	64.5	1.3
	τ_2	4.3	27.7		4.8	18.6		3.9	23.6		4.8	35.5	

[a] Percentage of probe domain with lifetime τ

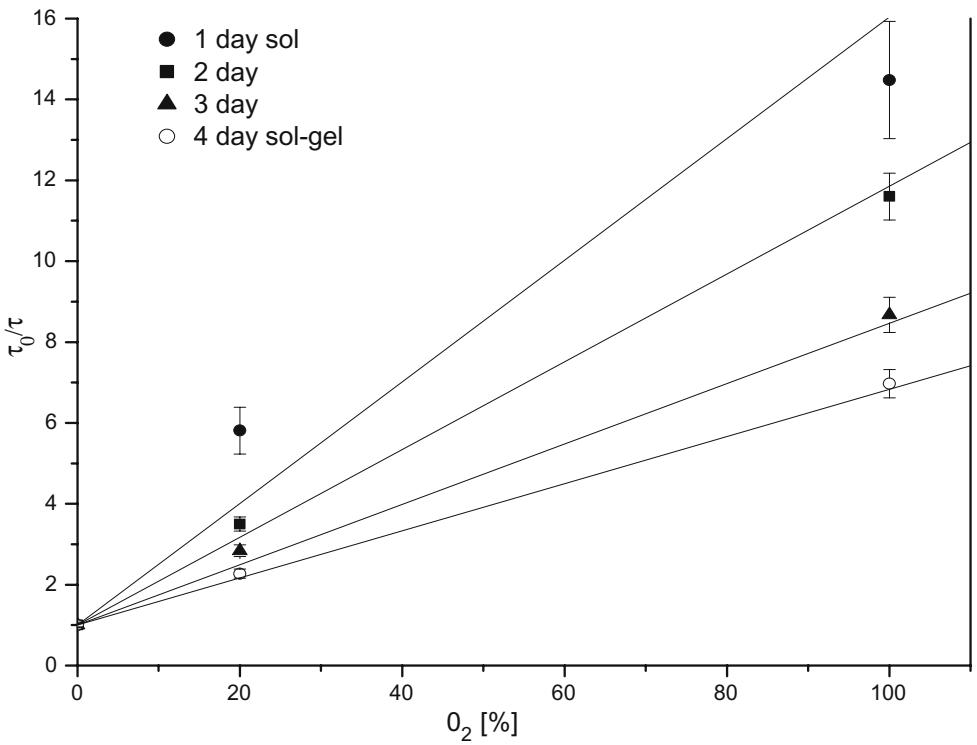

Fig. 8 Stern–Volmer plot for longer pyrene lifetime τ_1 on the consecutive days of gelation

Analysis of the data in the Table 3 leads to the conclusion that during the sol–gel transition in anaerobic conditions, the interaction of the changing microenvironment with the fluorophores result in a shortened fluorophore lifetime. Addition of oxygen to the gelling system, already in the amount of 20% oxygen content in the gaseous mixture, makes analysis of this impact impossible. The presence of a quencher causes that a dominating process is the quenching of fluorophore fluorescence because of the interaction with oxygen molecules, which is the same during the entire gelation process. Hence, it can be concluded that appearance of the gel lattice with pores filled with water and ethanol mixture does not affect significantly the diffusion of gaseous oxygen by this carrier. This is important from the point of view of the application of silane gel in the construction of optical sensors.

Other researchers, e.g., Soumillion et al. [16] also recorded the effect of the microenvironment of fluorophore molecules in the form of a gel lattice on the lifetime of this probe in the gel, its availability to the quencher, and the degree of quenching. A change in the silane monomer hydrolysis from acid to alkaline caused the formation of a gel with lower density and bigger pores. Pyrene, placed in this gel pores, was quenched by *o*-dicyanobenzene with K_{SV} four times higher than in the gel formed as a result of acid hydrolysis [16]. Significant for quenching of fluorophore molecules in the gel pores is the presence of water and ethanol molecules [13]. Bright et al. [13] carried out temperature studies of the quenching of ruthenium complexes, placed in TEOS-xerogel, by means of oxygen. In gel pores, below 150 °C, the fluorophores are surrounded by the molecules of water, which is sorbed on the pore surface, containing silanol groups -Si-0H. Above 150 °C, these groups are condensed on the surface of the pores, the solvent is removed from the gel cavities, accessibility of the fluorophore is enhanced, and the determined Stern–Volmer constant increases with increasing temperature [13].

Table 4 Stern–Volmer constants for pyrene quenched by oxygen on consecutive days of sol–gel transition determined on the basis of time-resolution measurements

Days	State of the system	K_{sv1} ($\%^{-1}$)	$k_{q1}\cdot10^{-5}$ ($\%^{-1}$ s^{-1})	R	K_{sv2} ($\%^{-1}$)	$k_{q2}\cdot10^{-5}$ ($\%^{-1}$ s^{-1})	R
1	Sol	0.15	9.93	0.986	0.001	0.07	0.895
2	Sol	0.12	8.49	0.990	0.004	0.33	0.852
3	Sol	0.08	9.68	0.999	0.003	0.33	0.838
4	Sol–gel	0.09	9.49	0.946	–	–	–

$K_{sv1}=k_{q1}\cdot\tau_{01}$, $K_{sv2}=k_{q2}\cdot\tau_{02}$; τ_{01}, τ_{02}—pyrene lifetimes on a given day of the gelling process without a quencher; k_{q1}, k_{q2}—bimolecular quenching rate constant

Figure 8 shows the results of the time-resolved measurements for τ_1 (Table 3) as a Stern–Volmer plot. The results have big errors because of problems in carrying out the experiment with a changing and thickening sol. A similar plot was obtained with τ_2. Constants K_{sv1} and K_{sv2} on the consecutive days of gelation estimated on the basis of Eq. 4 are given in Table 4. During the gelation process, the value of the quenching rate constant k_{q1} for pyrene molecules with decay time τ_1 remains similar, while the constant k_{q2} increases for the growing population of probe molecules having the short decay time τ_2. Besides, k_{q1} is several times higher than k_{q2}. This is an evidence of comparable rates of pyrene quenching by oxygen during the whole sol–gel transition. An increase in the population of pyrene molecules with the shorter decay time τ_2 and of their quenching rate is probably related to the formation of the gel lattice and appearance of additional interactions between the fluorophore and the silanol gel groups, including a possibility of fluorophore adsorption on the gel pore surface.

For comparison, Bright et al. [12] conducted fluorescence studies for pyrene in silane xerogel obtained from the TMOS monomer. They also distinguished two pyrene species entrapped in the gel lattice with different microenvironments. The researchers performed also steady-state and time-resolution fluorescence studies for pyrene in thin silane gel layers formed from the TMOS or TEOS monomer, directly on the optical fiber surface [22]. They produced their silane gel with a method different from ours, namely, as a result of a change in pH of TEOS hydrolyzed in different times. Results from steady-state fluorescence measurements showed that only one type of fluorophore centers were present in the gel and accessible for quenching by oxygen (linear relation according to Stern–Volmer). On the other hand, time-resolved fluorescence measurements showed that the best fit of the pyrene fluorescence decay in the thin gel layers on a fiber was given by a two-exponential function. Additionally, a slight effect of hydrolysis time on the value of K_{SV} and decrease in K_{SV} in the gel after a year of fiber storage was observed. The determined values of K_{SV} (Table 4) are several times smaller than the constants obtained for pyrene quenched by oxygen when the probe was chemisorbed on the aluminum surface by means of a long aliphatic chain [23, 24].

Summary

Pyrene placed in the silane sol is quenched during gelation process more by iodide ions than by acrylamide. The quenching has mainly a dynamic character and is controlled by diffusion. The rate constant of fluorophore quenching increases during sol–gel transition by one order of magnitude, using both quenchers, particularly for potassium iodide.

In the silane gel, the process of quenching by iodide ions and acrylamide is controlled by diffusion. The pyrene quenching in this carrier, formed into a block in the cuvette of the surface area 1 cm^2, is the quickest at the first of the two stages of quenching, i.e., up to 3 h.

Pyrene entrapped in the silane gel obtained by acid hydrolysis of TEOS is quenched by oxygen at a rate constant comparable to a constant determined in the input sol. This confirms good availability of oxygen to fluorophore molecules in the obtained carrier and a possibility of using a thin layer of this gel in the construction of a sensor or biosensor, which records changes in oxygen concentration.

Acknowledgments The authors are grateful to the Committee for Scientific Research (Poland) for a financial support through grant no. 4 TO8E OO9 24.

References

1. Gill I (2001) Chem Mater 13:3404
2. Miller E (2000) Wiadomoœci Chem 54(5–6):435
3. Miller E, Wysocki S, Jóźwik-Styczyńska D (2005) Annals Polish Chem Soc 1:564
4. Lu X, Winnik MA (2001) Chem Mater 13:3449
5. Pickup JC, Hussain F, Evans ND, Rolinski OJ, Birch DJS (2005) Biosens Bioelectron 20 9:2555
6. Bromberg A, Zilberstein J, Riesemberg S, Benori E, Silberstein E, Zimnavoda J, Frishman G, Kritzman A (1996) Sens Actuators B 31:181
7. Tsai H, Doong R (2005) Biosens Bioelectron 20 9:1796
8. Rowe CA, Tender LM, Feldstein MJ, Golden JP, Scruggs SB, MacCraith BD, Cras JJ, Ligler FS (1999) Anal Chem 71:3846
9. Petrou PS, Kakabakos SB, Christofidis I, Argitis P, Misiakos K (2002) Biosens Bioelectron 17:261
10. Andreou VG, Clonis YD (2002) Biosens Bioelectron 17:61
11. Miller E, Miller JS (2003) Colloid Polym Sci 281:745
12. Bonzagni NJ, Baker GA, Pandey S, Niemeyer ED, Bright FV (2000) J Sol-Gel Sci Techn 17:83
13. Baker GA, Wenner BR, Watkins AN, Bright FV (2000) J Sol-Gel Sci Techn 17:71
14. Sun Q, Tong Z, Wang Ch, Liu X, Zeng F (2003) European Polymer J 39:697
15. Wang H, Fang Y, Cui Y, Hu D, Gao G (2002) Mater Chem Physics 77:185
16. Jiwan J-LH, Robert E, Soumillion J-Ph (1999) J Photochem Photobiol A 122:61
17. Anandan C, Basu BB, Rajam KS (2004) European Polymer J 40:335
18. Schmidt H, Scholze H (1985) The sol–gel process for non-metallic inorganic materials. In: Fricke J (ed) Aerogels: proceedings of the First International Symposium. Springer, Wurzburg, Germany, p 49
19. Lakowicz JR (ed) (1999) Quenching of fluorescence. In: Principles of fluorescence spectroscopy. Kluwer, New York, p 237
20. Li L, Zhang Z, Long W, Tong A (2001) Spectrochim Acta A 56:385
21. Martinho JMG, Reis e Sousa AT, Oliveira Torres ME, Fedorov A (2001) Chem Phys 264:111
22. Dunbar RA, Jordan JD, Bright FV (1996) Anal Chem 68:604
23. Fujiwara Y, Amao Y (2003) Sens Actuators B 89:187
24. Fujiwara Y, Amao Y (2004) Talanta 62:655